

Concentration Effects in Partitioning of Macromolecules into Pores with Attractive Walls

Zuzana Škrinárová, Tomáš Bleha,* and Peter Cifra

Polymer Institute, Slovak Academy of Sciences, 842 36 Bratislava, Slovakia

Received May 24, 2002; Revised Manuscript Received September 17, 2002

ABSTRACT: The influence of polymer concentration on the partitioning of flexible macromolecules into adsorptive pores was examined by simulations in an open system under good solvent conditions. In dilute solutions, the partition coefficient $K(\epsilon, \phi)$ is sensitive to small variations of both polymer–pore attraction strength ϵ and concentration ϕ , whereas in semidilute solutions both influences level off. At weak attraction below critical adsorption energy ϵ_c , the coefficient K increases with ϕ in a fashion that resembles the weak-to-strong penetration transition found for purely steric exclusion ($\epsilon = 0$) but modified as if the width of pores effectively increased. At moderate attraction above the critical condition the increasing concentration brings about a dramatic drop in the value of K . Additionally, the $K(\phi)$ dependences in attractive pores were calculated by an approximate method based on expressions for chemical potentials, and the results were in good agreement with the simulation data. The critical adsorption energy ϵ_c for excluded volume chains was found to depend on concentration; the compensation point $K = 1$ was located at about $\phi = 0.012$ irrespective of the pore width. The energy and entropy contributions to the free energy of confinement were calculated and the compensation of their values at the critical condition was demonstrated. Furthermore, it was shown that the effect of concentration in polymer partitioning with adsorptive pores can alternatively be regarded as a confined adsorption and two alternatives of the adsorbed amount Γ were calculated. The adsorption and depletion concentration profiles $\phi_1(x)$ in the pore in equilibrium with the bulk solution were presented and their variation with concentration ϕ and attraction ϵ was analyzed.

Introduction

The equilibrium properties of flexible polymers confined within microporous disordered solids play an important role in a wide variety of applications. Pore cavities and capillaries are of vital interest for size exclusion chromatography, membrane filtration, colloid stabilization, catalysis, controlled drug release, clay-based nanocomposites, etc. Polymer chains when confined to a small space exhibit properties distinctly different from those in the unconfined space. Computer simulations of macromolecules in various simple geometries such as slit or cylinder can be employed to understand the static and dynamic properties of confined chains. For macromolecules confined between two parallel surfaces in a slit two thermodynamic conditions are distinguished:¹ (a) the number of polymer chains between plates is constant or (b) free exchange of molecules between confined and bulk solution is allowed (the cases of restricted or full equilibrium, respectively). The latter condition is appropriate for modeling of the partition equilibrium between flexible chains in a bulk solution and a pore.

The polymer partitioning is characterized by the partition coefficient, K , which is the pore-to-bulk concentration ratio at equilibrium, $K = \phi_1/\phi_E$. The theoretical models of partitioning of flexible macromolecules were recently reviewed.² In earlier treatment³ the pure steric exclusion of ideal chains in infinitely dilute solutions was addressed. The analytical approach³ based on the analogy between diffusion motion of a particle and conformation of a freely jointed polymer chain provided the relations for the partition coefficient K and the coil-to-pore size ratio $\lambda = R_g/D_p$, where R_g is the

radius of gyration of a chain and D_p is the characteristic dimension of a pore. According to these relations, the coefficient K depends on the ratio λ only and not on each of these two parameters taken separately. K is related to the free energy of confinement $\Delta A = -kT \ln K$, which represents a penalty for the transfer of a molecule from the bulk solution to the pore.

Purely steric partitioning of freely jointed and excluded volume chains into pores with repulsive chain–walls interaction was examined by Monte Carlo (MC) simulations.^{4–11} It was found that the Casassa partitioning rules for ideal chains³ have to be modified in the case of excluded volume chains to account for the solvent quality and solute concentration. These studies have shown that increasing the concentration of the polymer in the bulk solution increases the partition coefficient K above its value in the dilute limit K_0 . An existence of the weak-to-strong penetration transition, predicted already by de Gennes,¹² was confirmed in simulations^{1,7} in slits with repulsive walls and semidilute athermal solutions. The penetration into pores in semidilute solution is governed by the same scaling law as in dilute athermal solutions, only the nature of the scaling entity changes from the coil size to a size of the concentration blob. The change of solvent quality brings about a qualitative alteration of behavior: a delayed weak-to-strong penetration transition is found on increasing concentration in the Θ solvent. Here, repulsion between chains becomes effective in pushing the chains into pores at higher concentrations than in good solvents.⁸ The concentration effects were also studied in solutions of polymer mixtures with the aim to develop an effective technique for separation of macromolecules at higher concentrations.^{13,14}

The porous media used in partitioning experiments in many cases involve pore walls attractive to polymers.

* Corresponding author. E-mail: upoltble@savba.sk.

In such cases, polymer partitioning, alternatively sometimes termed confined adsorption, proceeds via a combined steric exclusion/wall-attraction mechanism. To explain this process, the diffusion-equation theory² of partitioning of ideal chains was extended^{15–17} to include a short-range segment–wall attraction potential ϵ . Partitioning of macromolecules in adsorbing pores is examined by theory^{15–19} and by simulations^{4,9,10} especially in order to clarify the separation mechanism in liquid chromatography of polymers. Attractive interaction of polymer segments with pore walls is a crucial feature in liquid adsorption chromatography. However, these interactions also contribute to some degree to the separation mechanism in real steric exclusion chromatography (SEC) of macromolecules on porous carriers. The combined effect of purely steric partitioning and wall attraction is particularly noticeable in critical chromatography^{20–23} operating close to the “critical” adsorption strength ϵ_c . Macromolecular solutes adsorb from solution onto a substrate if attractive potential ϵ exceeds the critical value ϵ_c (the adsorption/depletion threshold¹). Under critical conditions, the entropy loss due to chain confinement into the pore should be compensated for by the attractive energy gain, and the partition coefficient K may become independent of the chain length N of solute macromolecules (the compensation point).

Our previous simulations^{9,10} of partitioning of excluded volume chains into adsorptive pores treated athermal solutions in the dilute solution limit. In the present paper the partition coefficient K is calculated as a function of concentration in dilute, semidilute and concentrated solutions for weak and moderate attraction of polymer segments to the pore walls. The lattice MC simulations are performed in an open system that consists of a bulk solution in an equilibrium with a solution in a slit with two attractive plates. The results show that the pore–wall attraction governs partitioning only in very dilute solutions. In the rest of the concentration scale, the osmotic pressure in bulk becomes the driving force of the chain penetration into pore. For excluded volume chains, the adsorption/depletion critical conditions were found to depend on concentration. It was shown that the concentration dependence of the coefficient K in attractive pores can alternatively be regarded as a confined adsorption and quantified by the adsorption isotherms and concentration profiles across the pore.

Monte Carlo Simulations

The simulation procedure is based on direct equilibration between the slit and the free space and was described in previous papers.^{7–10} In simulations on a cubic lattice, two boxes connected to each other by the mouth of the slit are assumed: box E, representing the exterior (bulk) phase, and box I, representing the interior of the slit pore. Box E has dimensions of $50a \times 50a \times 30a$ (a is the lattice unit size) along the x , y , and z directions, respectively. In box I, with dimensions $(D + a) \times 50a \times 30a$ there are two solid walls at $x = a$ and at $x = D + a$, extending in the y and z directions and forming a slit. The width D is defined as the distance between the two lattice layers occupied by the solid walls. Polymer beads are not allowed to occupy the sites on the solid walls. Periodic boundary conditions apply to all pairs of opposite walls in the boxes except the solid walls. The mouth of the slit (the box I) is in contact with

the box E in the (x,z) plane at $y = 50a$ and, due to boundary condition periodicity, also at $y = 1a$. Boundary conditions used in the slit model provide the large (macroscopic) pore surface and the small separation of walls D .

Self-avoiding athermal walks consisting of $N = 100$ beads for each chain (up to 400 chains were used) were generated in the twin-box on a cubic lattice. The athermal model with zero value of the reduced contact energy $\epsilon_s = \epsilon_s/kT$, where ϵ_s is the segment–segment contact energy and kT the thermal energy, was used throughout and represents the good solvent condition. The restrictions on the chain conformations imposed by the lattice occupancy bring about the volume expansion of the coil resembling that of polymer chains in good solvents. Lattice vacancies implicitly represent athermal solvent molecules with zero segment–solvent interaction energy.

A short-range attraction interaction was assumed between the polymer segments and pore wall sites separated by one lattice unit. The reduced attraction energy per segment $-\epsilon = -\epsilon_w/kT < 0$ was a variable in the simulation, together with the slit width D and the concentration ϕ . The effective attractive potential $\epsilon_w = \epsilon_{pw} - \epsilon_{sw}$ can be considered as the difference between polymer–wall contact energy ϵ_{pw} and wall–solvent energy ϵ_{sw} (assumed to be zero in this model). The fraction of macromolecules within the slit having at least one contact with either of the walls, x_c , and the average number of wall-segment contacts counted per all chains in the slit, v_c , were also evaluated.

Chains were equilibrated using the reptation moves and the Metropolis algorithm. The simulations provide the equilibrium concentrations of the chains exchanged between the bulk and the slit without the need to calculate the confinement free energy from the respective chemical potentials. The overall thermodynamic ensemble is canonical but features the aspects known as the Gibbs ensemble, because it ensures that the chemical potentials of the chains in the slit and in the bulk are equal. The ratio of the volume fractions of the polymer in boxes I and E at equilibrium, ϕ_I/ϕ_E , gives the partition coefficient K . The chains in the intermediate regions with their parts belonging to both boxes I and E contributed all their segments either to the volume fraction ϕ_I or to ϕ_E , depending on where the majority of the chain segments is located. The volume fractions ϕ_E (denoted henceforth also as ϕ where appropriate) up to 0.45 were used. The segment density profiles across the slit, $\phi_I(x)$, were determined by averaging the segment concentration in each layer over many chain configurations. The root-mean-square radius of gyration of free unconfined chains of $N = 100$ is $R_g/a = 6.45$ in the dilute solution limit. The overlap concentration ϕ^* , representing a threshold between dilute and semidilute concentration regimes, was calculated using the relation⁸ $\phi^*[2^{1/2}(R_g/a + \alpha)]^3 = N$. Here, the extra constant $\alpha = 0.199$ accounts for the thickness of a coating needed to translate R_g^3 calculated on the lattice into the volume occupied by the chain in the continuous space. For athermal chains of length $N = 100$, $\phi^* = 0.120$.

Results and Discussion

Mapping the Surface $K(\phi, \epsilon)$. The dependence of the partition coefficient K on three variables, the bulk polymer concentration ϕ , the strength of attraction per

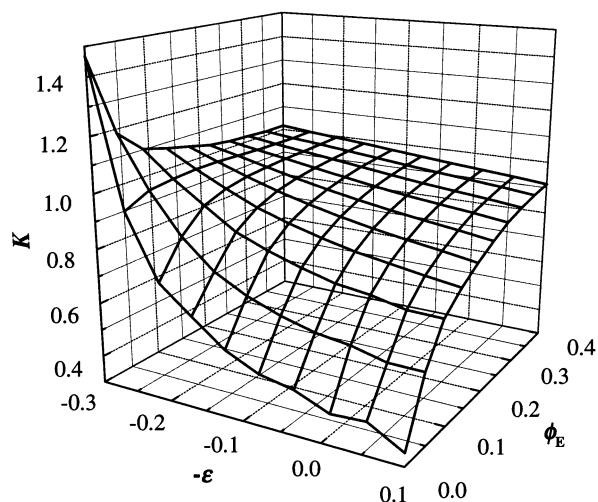


Figure 1. Partition coefficient K as a function of the attraction energy ϵ and of concentration ϕ_E for the slit width $D = 20$.

segment ϵ , and the slit width D have been examined. Simulations were performed for slit widths D/a between 8 and 40. The coil-to-pore size ratio, defined as $\lambda = 2R_g/D$, ranged between 0 and 1.6, thus fully covering the regions of weak ($\lambda < 1$) and moderate ($\lambda \approx 1$) confinements. Such a range of confinement is typical for experimental studies of partitioning of polymers in adsorptive porous glasses.²⁴

The variations of bulk volume fraction ϕ in simulations covered dilute, semidilute, and concentrated solutions. The regions of weak and moderate attraction of polymer segments to slit plates were examined, including the threshold value $\epsilon = \epsilon_c$ called the critical point of adsorption. The attractive potential $\epsilon = 0$ represents the pure steric exclusion where the polymer chains do not interact with the walls except the hard wall repulsion. It should be noted that ϵ is defined as the effective value of the preferential adsorption of a polymer on a surface relative to the solvent. Thus, polymer adsorption occurs only if the attractive segment-wall potential e_{pw} is more negative than the analogous potential of solvent molecules e_{sw} . The parameter ϵ can be linked to the χ_s parameter used in the self-consistent-field lattice models of adsorption.¹ Additionally, the parameter ϵ is related to the solvent strength concept of Snyder²⁵ employed in chromatography to correlate the adsorption behavior of solutes in various solvents on silica or other substrates. The variations of the parameter ϵ are inversely proportional to the temperature changes.

So far the effects of concentration and pore wall attraction on the partition coefficient K were treated separately in simulations. For example, the functions $K(\phi)$ for purely steric exclusion and the function $K(\epsilon)$ in dilute solution limit were computed¹⁰ for various slit widths D . Interestingly, both variables ϕ and ϵ independently influence the partitioning curve K vs λ in a similar way: the partitioning of chains of a given size R_g is enhanced by an increase in concentration or attraction strength,¹⁰ as if the pore width effectively grew with increasing ϕ or ϵ .

Simulations by parallel variations of both parameters ϕ and ϵ provide the functions $K(\phi, \epsilon)$ at various pore widths D . The characteristic form of the surfaces $K(\phi, \epsilon)$ is illustrated in Figure 1 for $D = 20$ (the confinement ratio $\lambda = 0.645$). A marked variation in the shape of the graph is noticeable in the region of dilute solutions.

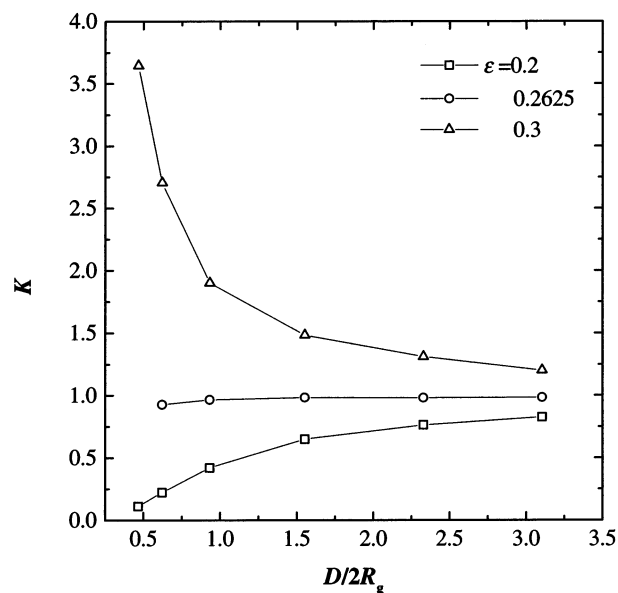


Figure 2. Partition coefficient K as a function of the reduced slit width $D/2R_g = 1/\lambda$ at infinite dilution ($\phi_E \approx 0.001$) for three different values of the attraction energy ϵ .

Here, the value of the coefficient K is susceptible to small variation of either of the parameters ϕ or ϵ . However, in the semidilute solution, above the overlap concentration, $\phi^* = 0.120$, the surface levels off and a broad quasi-plateau is formed (Figure 1). In this region the influence of attraction strength ϵ on the coefficient K is much suppressed and the coefficient K moves toward unity with an increase of ϕ . Figure 1 includes data for negative values of the parameter ϵ . Such an enhanced segment-wall repulsion actually embodies the reduction in the number of accessible lattice layers, as if the pore width D effectively decreased. Overall, it is evident from Figure 1 that it is not possible to construct the function $K(\phi, \epsilon)$ by a simple addition of two single-parameter functions $K(\phi)$ at $\epsilon = 0$ and $K(\epsilon)$ at $\phi \rightarrow 0$.

A prominent feature of Figure 1 is the presence of a "peak" in the region of moderate wall attraction $\epsilon > \epsilon_c$ for very dilute solutions. In this region, polymer segments adsorb on the walls, and the coefficient $K > 1$. Here, the wall attraction potential represents a driving force of partitioning, which "pulls" the chains into the pore and offsets the steric exclusion (confinement) blockage. At the critical point of adsorption ϵ_c , the transition from depletion to adsorption regime occurs. Earlier, the critical condition in this system was estimated⁹ on the assumption that ϵ_c occurs at the point where $K = 1$ and steric exclusion is offset by the adsorption effects. For athermal excluded volume chains the compensation point was found⁹ at $\epsilon_c = 0.2625$ for $N = 100$. Below this point, in the region of weak attraction, $0 < \epsilon < \epsilon_c$, polymer chains become depleted from the walls and $K < 1$ in Figure 1, even though the K values are still enhanced relative to the purely steric exclusion.

The graphs of function $K(\phi, \epsilon)$ for smaller or larger pore widths are qualitatively similar to Figure 1. The peaks in functions $K(\phi, \epsilon)$, i.e., partition coefficients in the region of very dilute solutions above critical energy, increase with decreasing $D/2R_g$, the pore width reduced by the coil diameter (Figure 2). Evidently, the pulling of chains into pores by attractive walls becomes more effective in narrow slits. In the subcritical region, the

changes of K with D in dilute solution limit are controlled by the confinement penalty. Near the critical condition ϵ_c the coefficient K at $\phi \rightarrow 0$ seems to be independent of the pore size, except at small D (Figure 2).

The majority of chains in the pore exhibit at least one contact with the pore walls and the population of such chains is specified by the fraction x_c . The remaining fraction $x_f = 1 - x_c$, are free molecules floating near the pore center. For example in a pore of $D = 12$ in the dilute solution limit, $x_f = 19.0$, 7.6 , and 1.6% of floating chains for $\epsilon = 0.1$, 0.2 , and 0.3 , respectively. Obviously, the fraction x_f increases in wide pores. For instance, there are more free than adsorbed chains in dilute solutions in the pore of $D = 40$ at $\epsilon = 0.3$. In contrast, in narrow pores macromolecules build up contacts with both slit plates and if $\epsilon > \epsilon_c$ they form intrapore bridges. As a result, the volume fraction inside the pore ϕ_1 can be divided into contact chains (f_1^c) and free chains (f_1^f) parts. Above the adsorption threshold the term f_1^c accounts for chains located in the adsorbed layer. In the same vein, the overall partition coefficient K can be expressed as $K = K^c + K^f$.

A minimum of $n_l = 30$ chains of the length $N = 100$ is needed to fully cover the available surface area of two slit plates $2 \times 30 \times 50 = 3000a^2$ in case that all the chain segments are adsorbed. In fact, instead of 100 segments, only about 21 segments of an average chain in a slit are adsorbed at $\epsilon = 0.3$ in a pore of $D = 12$ at dilute limit (Figure 3a). Thus, a number of chains greater than 30 is needed to attain the full surface coverage of the plates. The average number of contacts per chain in the slit ν_c and the fraction of chains in the slit in contact with the wall x_c diminishes with a decrease of the attraction potential ϵ (Figure 3a). Increasing concentration ϕ brings about competition of chains for wall contacts, which differ in the region below and above the adsorption threshold. In the adsorption region, the number of adsorption contacts is at a maximum in the dilute solution limit (Figure 3a); very tight adsorption of chains on the surface arises.²⁶ This adsorption draw of chains into the pore diminishes with increasing ϕ . In contrast, increasing ϕ enhances the tendency to form contacts in the subcritical region.

Effect of Concentration on K . The concentration effect in partitioning is shown in Figure 3b for some representative values of the attraction potential ϵ and slit width $D = 8$. The simulation data at the bottom of Figure 3b correspond to partitioning by purely steric exclusion. The behavior in this region was thoroughly analyzed in previous papers dealing with athermal and Θ solutions.^{7,8,13,14} A slight penetration of chains into a pore in the dilute regime changes into strong penetration in the semidilute regime and subsequently into saturation. The primary driving force for this behavior is the bulk solvent nonideality, first in the bulk solution and then in the pore solution.²⁷

In the range of attraction potentials $0 < \epsilon < \epsilon_c$, the steric exclusion effect prevails over the wall-attraction effect. The partition coefficient at infinite dilution K_0 increases with the attraction potential ϵ as if the width of the corresponding pores effectively increased (Figure 3b). Similarly, the entire concentration range for the weak attraction $\epsilon = 0.2$ follows a pattern of that for purely steric exclusion, but modified by the widening of pores. As a result, the penetration transition in Figure 3b becomes less pronounced in this case and a rapid

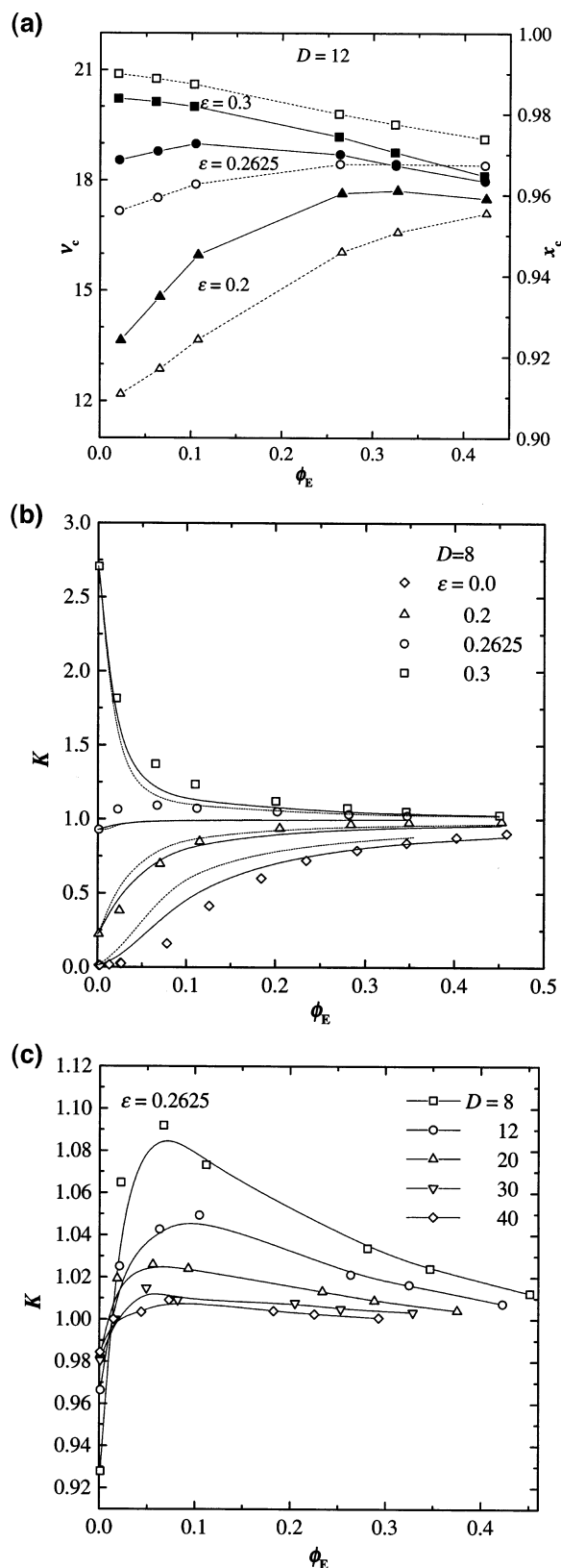


Figure 3. (a) Effect of concentration ϕ_E on the average number of contacts per chain in slit, ν_c (open symbols, dashed lines) and on the fraction of macromolecules with contact with either of the walls, x_c (full symbols, solid lines), for the slit width $D = 12$ and $\epsilon = 0.2, 0.2625$, and 0.3 . (b) Effect of concentration ϕ_E on the partition coefficient K for $D = 8$ and variable ϵ , data from Monte Carlo simulations. Flory and Huggins theories are shown with symbols, dotted lines, and full lines, respectively. (c) Variation of the partition coefficient K with ϕ_E at the critical condition $\epsilon = 0.2625$ for different slit widths D .

leveling off to $K = 1$ takes place. Osmotic-pressure-induced drive of molecules into the pore also explains the increase in the average number of wall contacts per chains ν_c with ϕ for $\epsilon = 0.2$ seen in Figure 3a.

Above the adsorption threshold, the effect of wall attraction prevails over steric exclusion. In this region the concentration effect on K features a dramatic drop in K values occurring already in very diluted solution. Nevertheless, the coefficient K still remains $K > 1$ and slowly levels off to about unity in semidilute solutions. In a way, this behavior represents a transition from an extreme penetration to a high penetration of molecules into the pore. The intrapore pulling effect, operative in very dilute solutions is drastically reduced by the concentration ϕ . This comes about because the long-range cooperative effect of segment adsorption in the dilute regime is screened by mutual interpenetration of coils on increasing concentration in the semidilute regime. With an increase in ϕ , the osmotic pressure in bulk solution pushes the molecules into the pore, thus increasing the intrapore concentration ϕ_I . Accordingly, in the push–pull (or $\phi - \epsilon$) balance shaping the K value, the chain repulsion effect turns out to be prevailing even in dilute solutions.

In steric partitioning the concentration dependence of K in dilute solutions is frequently treated by the virial expression

$$K = K_0(1 + \kappa_1\phi + \kappa_2\phi^2 + \dots) \quad (1)$$

where K_0 , κ_1 , and κ_2 depend on the confinement ratio λ . Measurements of partitioning of dilute solutions of flexible polymers under static conditions^{28–30} show that in good solvents the first virial coefficient κ_1 is positive and the coefficient K increases with bulk concentration ϕ . The same conclusion ensued from the concentration dependence of K measured by dynamic partitioning in SEC, specifically, from the shift of the peak elution volume V_e with the concentration c of the injected volume.³¹ Porous media usually employed in partitioning measurements, such as controlled pore glasses, are surface-treated or coated to inhibit the adsorption of solutes. Nevertheless, a purely steric mechanism of partitioning can hardly be expected in these cases and some minor contribution of segment–wall attraction can be expected. Thus, the simulation results for the weak potential ϵ from the range $0 < \epsilon < \epsilon_c$ in Figure 3b, instead of the results for $\epsilon = 0$, should be utilized in appraisal of the experimental data on porous glasses. In the case of attractive pores the parameters in eq 1 depend on both λ and ϵ values. The simulation data in Figure 3b indicate that κ_1 and κ_2 terms may not vanish even at the compensation point.

A comprehensive theory of combined steric-exclusion/wall-attraction partitioning of excluded volume chains at finite concentrations has not yet been developed. Existing approaches are limited to hard sphere particles³² or to ideal chains and/or to infinite dilution.^{15,16,18,19} Hence, a simplified approach is used in the following to calculate the concentration dependence of K in attractive pores. The chemical potentials of macromolecules in bulk solution, μ_E , and in the pore, μ_I , are equal at equilibrium. The potential μ_E depends on the polymer concentration ϕ_E only. The intrapore chemical potential holds an analogous concentration term $\mu_I(\phi_I)$, but additionally, it involves terms representing the free energy change of a single chain due to the confinement

penalty $\Delta A^+_{\text{conf}}(\lambda) > 0$ and the attraction gain $\Delta A^+_{\text{att}}(\epsilon) < 0$:

$$\mu_E(\phi_E) = \mu_I(\phi_I) + \Delta A^+_{\text{conf}}(\lambda) + \Delta A^+_{\text{att}}(\epsilon) = \mu_I(\phi_I) - kT \ln K_0 \quad (2)$$

It is assumed that these two free energy terms are a function of the respective parameters λ or ϵ only and are independent of the intrapore concentration ϕ_I . Their sum is effectively represented by the term $-kT \ln K_0$ ascertained in very dilute solutions. Thus, in this simplified approach, the confinement and adsorption effects on the concentration dependence of K are inseparable. By using a suitable function for the concentration terms $\mu_E(\phi_E)$, $\mu_I(\phi_I)$ and choosing the value of K_0 , one can calculate the concentration dependence of the partition coefficient K , assuming a homogeneous concentration in pores.

In the lattice model with the lattice coordinate number Z , the sites are occupied by polymer chains consisting of N consecutive sites and solvent molecules, each occupying a single site. A positive contact energy ϵ_s is assigned when chain segment and solvent molecule are next to each other on the lattice. In the Flory model,³³ the free energy of mixing ΔA^m_F of the polymer solution is given as

$$\frac{\Delta A^m_F}{n_{\text{site}}kT} = \frac{\phi}{N} \ln \phi + (1 - \phi) \ln(1 - \phi) + (Z/2 - 1) \frac{\epsilon_s}{kT} \phi(1 - \phi) \quad (3)$$

where n_{site} is the number of lattice sites in the system. Here the bonded contacts were excluded from the interaction term. In the Huggins model,³⁴ the free energy of mixing ΔA^m_H is given as

$$\frac{\Delta A^m_H}{n_{\text{site}}kT} = \frac{\phi}{N} \ln \phi + (1 - \phi) \ln(1 - \phi) - \frac{Z}{2} (1 - \alpha\phi) \ln(1 - \alpha\phi) + \frac{Z}{2} \frac{(1 - \alpha)\epsilon_s}{kT} (1 - \phi)q \quad (4)$$

where $\alpha = 2Z^{-1}(1 - N^{-1})$ and $q = (1 - \alpha)\phi/(1 - \alpha\phi)$. The change of the chemical potential of polymer to be used with eq 2 for either of the above two free energies of mixing is given by

$$\Delta\mu/N = \Delta A^m(\phi) + (1 - \phi) \partial \Delta A^m(\phi) / \partial \phi \quad (5)$$

The resulting expressions for the chemical potential of a polymer in athermal solvents with vanishing interaction term read

$$\frac{\Delta\mu_F}{NkT} = \frac{1}{N} \ln \phi + (1 - \phi) \left(\frac{1}{N} - 1 \right) \quad (6a)$$

$$\frac{\Delta\mu_H}{NkT} = \frac{1}{N} \ln \phi - \frac{(1 - \alpha)}{\gamma} \ln(1 - \alpha\phi) \quad (6b)$$

The concentration dependences of K in the case of attractive pores obtained by the above-described procedure are shown in Figure 3b for the slit of $D = 8$. Both expressions according to Flory and Huggins for the concentration dependence of the chemical potentials were employed. The $K(\phi)$ functions predicted by this procedure are quite similar to the MC results for all

three attraction strengths selected. Both analytical lattice models predict stronger dependence of K on concentration than the simulation results since they overestimate the osmotic pressure.³⁵ In this respect, the data in Figure 3b show that the Huggins approximation is more appropriate, as already observed.^{35,36} The overall agreement of the $K(\phi)$ curves from theory and from simulations lends support to the assumption of independence of the attraction term $\Delta A_{\text{att}}(\epsilon)$ from concentration.

The Critical Condition. The notion of critical condition in polymer partitioning into attractive slits arises from the adsorption transition of an ideal single chain near a solid wall. At the critical point of adsorption ϵ_c , attractive interaction counterbalances the polymer-wall excluded volume effect. The value ϵ_c in the limit of infinite chain length can be termed¹⁸ the adsorption Θ point by the analogy to the conventional Θ point in polymer solutions. For a chain of large molecular weight, a sharp adsorption transition at a solid wall is supposed. In partitioning of macromolecules into adsorptive pores, the critical condition is taken to be the same as the critical adsorption point ϵ_c of a single chain near an adsorbing surface. Furthermore, it is assumed^{15,18} that for ideal linear chains at the critical condition the partition coefficient $K = 1$ and is independent of chain length N .

Computer simulations allow to assess the critical condition in the case of real macromolecules of finite lengths, similar to that encountered in critical chromatography experiments. As a rule, the mentioned idealized conditions are not satisfied here: the compensation of steric exclusion and adsorption terms is not governed by the single value parameter ϵ_c and the adsorption transitions are flattened. Instead, the compensation point may in this case depend also on other variables, such as the chain length and concentration. In previous simulations,⁹ the critical point ϵ_c of excluded volume chains of finite lengths in an equilibrium with an adsorptive slit was estimated as the value of ϵ at which the coefficient $K = 1$ and steric exclusion and wall attraction effects are compensated. A weak chain-length dependence of the compensation point $K = 1$ was detected,⁹ contrary to the ideal chain results,^{15,18} which predicted the compensation point $K = 1$ to be independent of N . The value $\epsilon_c = 0.2625$ was found⁹ to be appropriate for chain lengths in the range of N from 70 to 110.

Polymer-polymer interactions were so far ignored in the theory and simulations of partitioning of nonideal chains at critical conditions. The simulation data for in Figure 3b indicate that the critical condition for excluded volume chains in slit may slightly depend on the concentration ϕ as well. In Figure 3c, the variation of K with ϕ at critical condition $\epsilon_c = 0.2625$ is presented in more detail for various pore sizes. For all pore widths, the concentration dependence of K shows a maximum which is most pronounced for $D = 8$. At very small concentrations, the K values are below unity for all pore widths. The functions intersect close to coordinates $\phi = 0.012$ and $K = 1$ which may define the compensation point, independent of pore width D , in this system.

A tentative explanation of the maximum in Figure 3c can be attempted. On increasing concentration the chains start to behave collectively near the attractive slit walls. Though the concentration in bulk may be below ϕ^* , the concentration is higher at attractive walls.

The weakly adsorbed chains support each other at the wall by their entanglements and that lead to an increase in K . This small effect dies out around $\phi^* = 0.120$, where the penetration of chains due to osmotic pressure starts to predominate and K levels off. The effect leading to this maximum is not specific to the compensation point only, but it is noticeable here since both below and above ϵ_c it is overshadowed by the strong concentration dependence of K .

The specification of critical conditions for excluded volume chains in a slit is a matter of debate.^{23,37} The critical adsorption point was redefined²³ for asymptotically long chains as a point where change in the free energy of confinement per one segment $\Delta A/N$ vanishes at $N \rightarrow \infty$. It was argued^{15,37} that the coefficient K need not be unity for a single excluded volume chain at the critical point, but its value depends slightly on the slit width and the chain size. At finite concentrations, location of the critical energy is a matter of delicate balance of the intra- and intermolecular excluded volume effects and judging from Figure 3c, specification of both N and ϕ is needed. Nevertheless, the weak N and ϕ functions of the partition coefficient under critical conditions may be unimportant for practical purposes in critical chromatography. A weak concentration dependence of the critical condition should be connected to the concentration variations of the functions ν_c and x_c in Figure 3a for $\epsilon_c = 0.2625$. It is also apparent in Figure 2 where the majority of curves intersect at $K = 1.036$ for $\epsilon_c = 0.2625$. Sometimes a noticeable change in the number of contacts at ϵ_c is intuitively expected: below the critical adsorption energy most of the polymer segments are supposed to avoid the surface whereas above this critical condition the chains should have many contacts with the substrate. Actually, the data in Figure 3a show that the average number of contacts ν_c changes gradually near the critical condition.

Entropy and Energy Contributions to Partitioning. The concentration dependence of other thermodynamic functions of partitioning is of interest. The adsorption energy of macromolecules in a slit is given as a product of segmental sticking energy and the average number of contacts with the wall per chain in a slit, $\Delta U = -\nu_c \epsilon$. By a combination of this energy term with the free energy of confinement $\Delta A = -kT \ln K$, the entropy term $T\Delta S$ can be evaluated. These terms are shown as a function of ϕ in Figure 4 for a slit of $D = 20$. The opposite trends below and above ϵ_c in the average number of contacts as a function of ϕ (Figure 3a) are transmitted to the respective trends of the adsorption energy $\Delta U/kT$ and entropy $\Delta S/k$ in Figure 4. Thus, an increase in attractive stabilization by ϕ of the ΔU term in the subcritical region changes to an analogous decrease in the supracentric region. As evident from Figure 4, the free energy ΔA is given by the difference of the rather large (in absolute value) energy and entropy terms.

The energy and entropy terms should be fully balanced at the compensation point $K = 1$ near the critical condition ϵ_c . Figure 5 shows this compensation as a function of plate separation D for two values of concentration $\phi = 0$ and 0.1 approximately corresponding to the lower and upper bounds of K values in Figure 3c. The entropy term $\Delta S/k$ in Figure 5 represents the loss of entropy of polymers on the confinement. The reduction of entropy is brought about by two factors:¹⁰ (a) a loss of molecular orientation entropy due to preferential

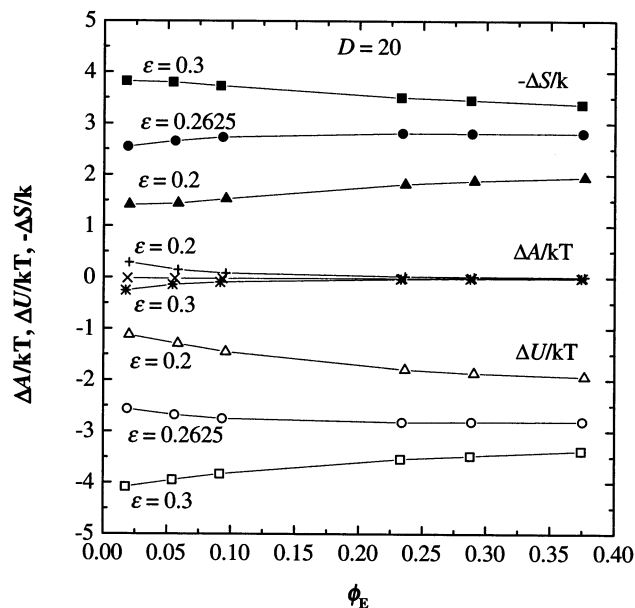


Figure 4. Changes in the free energy of confinement $\Delta A/kT$, the entropy $-\Delta S/k$, and the adsorption energy $\Delta U/kT$ with concentration ϕ_E in a slit of $D=20$ for three attraction energies ϵ .

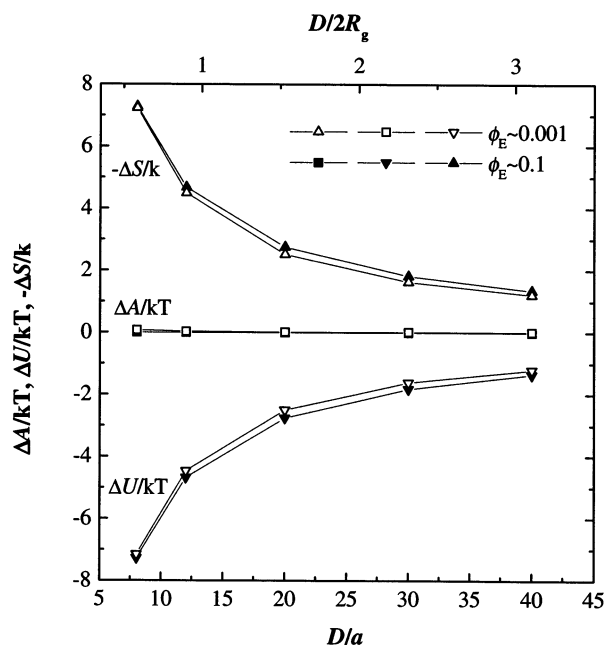


Figure 5. Changes in $\Delta A/kT$, $\Delta S/k$, and $\Delta U/kT$ as a function of slit width D at the critical energy $\epsilon = 0.2625$ at two concentrations.

alignment of long axis of chain ellipsoids along the pore walls and (b) a loss of entropy by a loss in the number of conformations allowed for a chain in a pore. The latter mechanism, elimination of disallowed conformations, actually represents an effective deformation of the intrinsic shape and mean dimensions of the coils due to the presence of pore walls. The extent of chain distortion depends on the pore width D and on the surface interaction, for example, more strongly adsorbed chains exhibit tighter forms²⁶ with more train sequences, shorter loops and free ends, etc. This phenomenon as well as the suppression of free (nonadsorbed) chains accounts for an increase in the energy term $\Delta U/kT$ in narrow slits at the compensation point (Figure 5). One can expect that the drop in energy with

decreasing D will be reversed in very narrow pores unable to accommodate the chains, and the $\Delta U/kT$ term will rise sharply.

Confined Adsorption Characteristics. The equilibrium distribution of solutes between bulk solution and adsorptive porous materials can alternatively be treated as a confined adsorption using quantities employed in the studies of the adsorption on flat surfaces. In confined adsorption, again, a combined mechanism of adsorption to internal pore walls (dominant effect) and of pore confinement is presumed.²⁴ Such description applies for example for porous glass beads without a surface treatment; the silanol groups in beads are frequently masked by a reaction with silanes in order to prevent the surface adsorption.

Instead of the partition coefficient K , the key parameter in confined adsorption is the adsorbed amount of polymer in equilibrium with the bulk phase, Γ^a . The adsorbed amount for a polymer near a surface is defined¹ in terms of contributions to the volume fraction profile $\phi_I(x)$, the variation of ϕ_I with the distance from the surface x . For a pore–bulk solution equilibrium, the adsorbed amount can be characterized by the total number of segments belonging to the chains inside of the pore, $n_I N$, divided by the area of both adsorptive plates of the slit

$$\Gamma^a = n_I N / 2A = \phi_I(D-1)/2 = K\phi(D-1)/2 \quad (7)$$

Here, n_I is the number of chains of $N = 100$ segments within the pore of the width D of the $D - 1$ available layers. In our model both internal walls of the slit contribute to the surface area $2A$. The volume fraction inside the pore, ϕ_I , refers to both adsorbed (by a minority of segments) and free chains. The adsorbed amount can be expressed in units of polymer mass per surface area by multiplication of Γ^a with ρ , the partial density of the polymer. The latter equation connects the adsorbed amount with the partition coefficient. Since Γ^a refers to both adsorbed and free-floating intrapore chains, it characterizes the polymer uptake by both intrapore “surface” and “volume” adsorption, respectively. The corresponding adsorbed amounts $(\Gamma^a)_S$ and $(\Gamma^a)_V$ can be introduced, if desired.

The variation of the adsorbed amount Γ^a with ϕ is shown in Figure 6a for two pore sizes. The adsorption isotherm for $\epsilon = 0.3$ shows at first a concave curvature in the dilute regime and then, as ϕ goes into the semidilute concentration range, the isotherm rise in almost a linear way. These two parts of the isotherm mirror the two regions, drop down and leveling-off, in the $K(\phi)$ functions in Figure 3b. The adsorbed amount $\Gamma^a = 1$, i.e., one intrapore polymer segment per unit surface area (a^2), formally corresponds²⁶ to one “monolayer”. An apparent “multilayer adsorption” is seen in Figure 6a at higher ϕ . The adsorbed amount Γ^a is positive at any time, when the coefficient $K > 0$ at partitioning, even in the region below the adsorption threshold. Below ϵ_c the depletion polymer–wall interaction is manifested by the convex type of isotherms in dilute solution (Figure 6a).

The excess adsorbed amount Γ^{ex} can be arbitrarily introduced by replacing the intrapore volume fraction ϕ_I by the difference $\phi_I - \phi_E = \Delta\phi = \phi(K - 1)$ in the above equation:

$$\Gamma^{ex} = \phi(K - 1)(D - 1)/2 \quad (8)$$

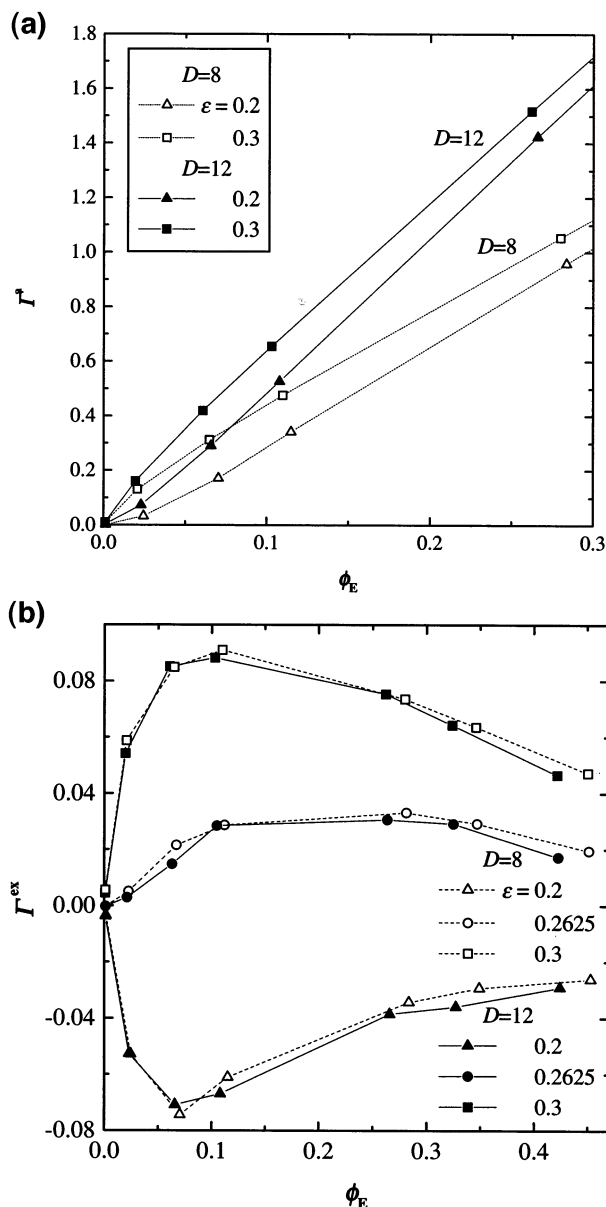


Figure 6. Adsorbed amount Γ^a (a) and the excess adsorbed amount Γ^{ex} (b) as a function of concentration ϕ_E for two different slit widths $D = 8$ and 12 and attraction energies $\epsilon = 0.2$ and 0.3 .

Figure 6b shows the excess isotherms Γ^{ex} for two pores $D = 8$ and 12 at three values of ϵ . Above the adsorption threshold, at $\epsilon = 0.3$, $\Gamma^{ex} > 0$ and its variation with ϕ looks like the low-affinity type of isotherm. The rising part of this isotherm corresponds to a drop in the $K(\phi)$ function in Figure 3b in the region where attractive pull is still potent. The maximum in the isotherm in Figure 6b is located approximately at the bulk overlap concentration ϕ^* . The decreasing part of the Γ^{ex} isotherm is a sign of the bulk osmotic pressure effect. The excess isotherm Γ^{ex} at energy ϵ_c approximating the critical condition exhibits a small positive adsorption, in accordance with the plots of the $K(\phi)$ functions in Figure 3c. In the region of the weak attraction strength the depletion isotherms, $\Gamma^{ex} < 0$, are observed (Figure 6b). In all cases the excess isotherms seem not to be affected by the pore width.

Concentration Profiles. Adsorbed amounts in eqs 7 and 8 are defined through the intrapore concentration ϕ_I averaged over the whole pore width. The spatial

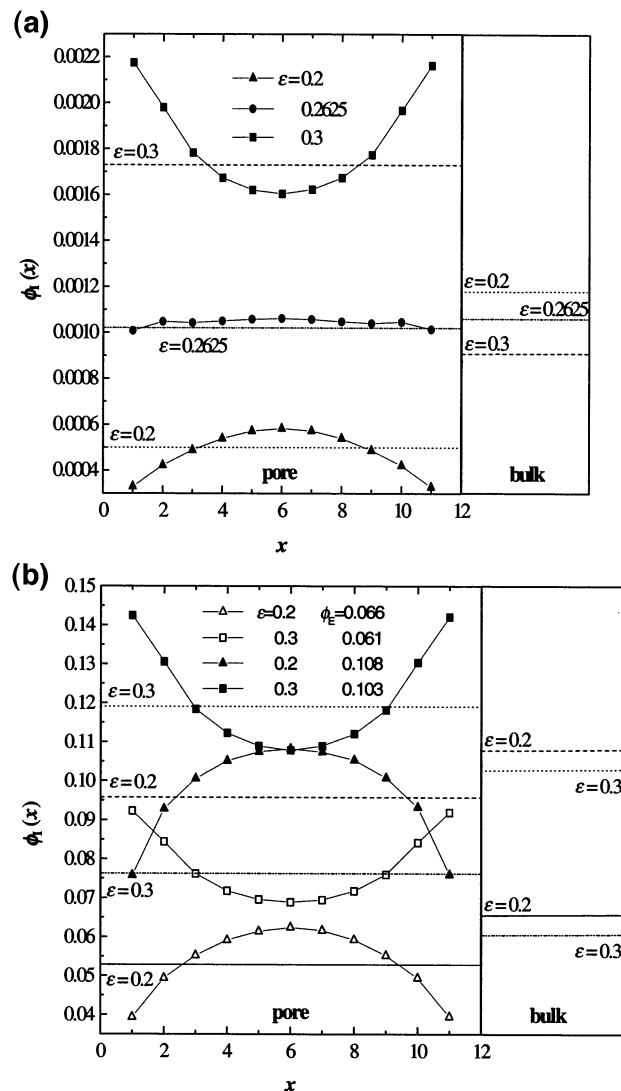


Figure 7. Concentration profiles $\phi_I(x)$ in the slit of $D = 12$ and average concentrations (shown by horizontal lines) in a slit, ϕ_I , and in bulk, ϕ , calculated for variable attraction energies in the infinitely dilute solution limit (a) and for two concentrations in the dilute solution range (b).

distribution of polymer segments as a function of the distance x from the pore walls is given by the segment concentration profile $\phi_I(x)$. From these concentration profiles both adsorbed amounts, Γ^a and Γ^{ex} , can alternatively be evaluated. In contrast to concentration profiles characterizing polymer solutions near a planar surface, an additional parameter, the external concentration ϕ , has to be specified in the case of a pore–bulk solution equilibrium. Concentration profiles in very dilute solutions ($\phi_I \approx 0.001$) in the slit of $D = 12$ are shown in Figure 7a for three attraction potentials, together with the average intrapore concentration ϕ_I . A gradual change from a depletion layer to an enrichment layer with an increase in ϵ is apparent in the form of these profiles. The profile $\phi_I(x)$ is more or less flat at the potential ϵ_c ; i.e., at the critical condition the segment concentration is independent of the distance from the pore walls.

Adsorption and depletion concentration profiles $\phi_I(x)$ in the slit of $D = 12$ at two concentrations in the dilute solution range are shown in Figure 7b. Since the molecule and the pore have similar dimensions ($\lambda = 1.074$), the depletion or enrichment layers from both

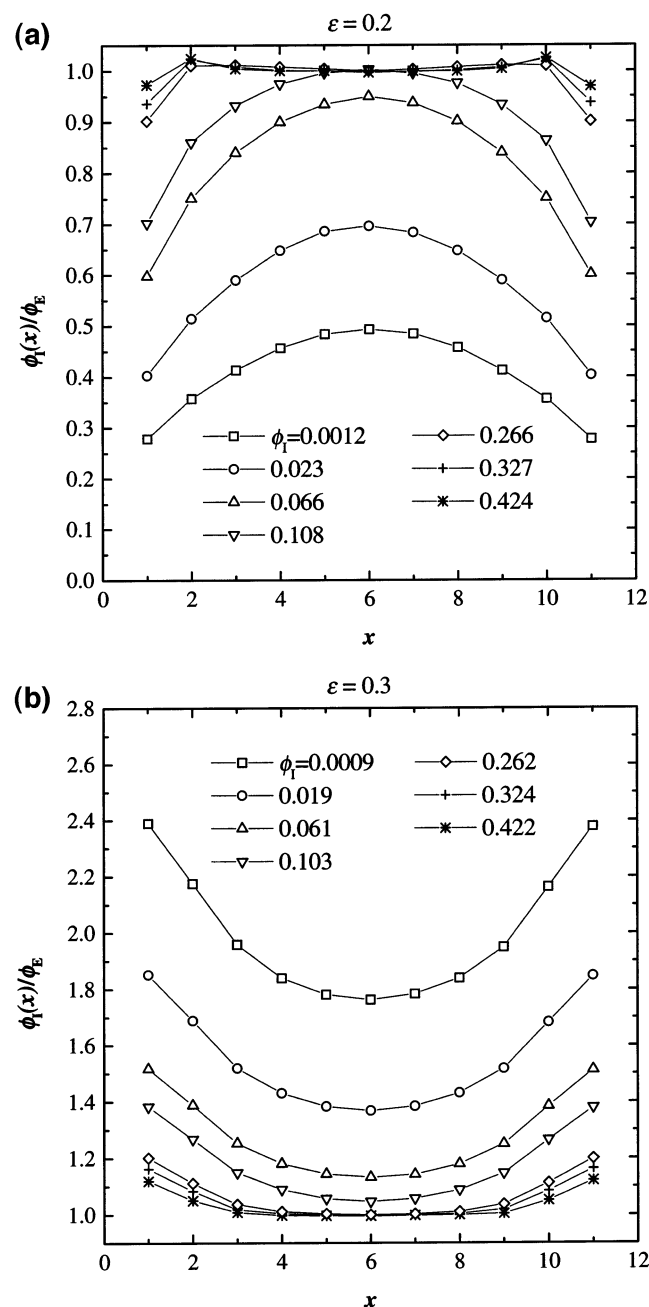


Figure 8. Normalized concentration profiles $\phi_I(x)/\phi$ in the slit of $D = 12$ and of attraction energy $\epsilon = 0.2$ (a) and $\epsilon = 0.3$ (b) calculated for the concentrations ϕ specified in the figure.

plates extend up to the pore center. Hence, no flat portion of the profile in the middle of the slit is seen, and the volume fraction in the center differs from the average intrapore concentration ϕ_I .

The variation of the relative segment concentration profiles $\phi_I(x)/\phi_E$, or the "layer" partition coefficient $K(x)$, in a wide concentration range is presented in Figure 8 for the slit of $D = 12$. As the concentration builds up at depletion conditions ($\epsilon = 0.2$), the chains become distributed more uniformly in the slit and the depletion layer is filled up. At high concentrations the normalized profiles in Figure 8a exhibit shoulders due to a layering structure that develops near the pore walls.³⁸ The local partition coefficient $K(x)$ in shoulders is enhanced to values over unity. As a result of segment ordering, a shallow basin is present in the middle, quasi-flat portions of normalized profiles.

The variation of normalized profiles with concentration under adsorption condition ($\epsilon = 0.3$) is shown in Figure 8b. The concentration profiles flatten with ϕ : enrichment layers become less pronounced, and the local partition coefficient $K(x)$ in the pore center rapidly diminishes with increasing concentration. Extrapolation of data in Figure 8b to the concentration limit of $\phi = 1$ indicate that an almost completely flat concentration profile can be expected for a polymer melt within adsorptive pores. The strength of polymer–wall attraction should have a minute impact on the profile, restricted to a thin zone near the walls.

Conclusions

The influence of polymer concentration on the partitioning of flexible macromolecules into adsorptive pores was examined by simulations in an open system under good solvent conditions. The results show that in dilute solutions the partition coefficient $K(\epsilon, \phi)$ is sensitive to small variations of either polymer–pore attraction strength ϵ or concentration ϕ . The penetration of molecules into the pore in dilute solutions is controlled by both adsorption draw and bulk osmotic pressure push. In semidilute solutions, the value of the coefficient K is determined mainly by the concentration factor. At weak attraction below the critical adsorption energy ϵ_c , the function $K(\phi)$ resembles the weak-to-strong penetration transition found for purely steric exclusion ($\epsilon = 0$) but modified as if the width of pores effectively increased. At moderate attraction above the critical condition the increasing concentration brings about a striking drop in the value of K . A method to calculate the $K(\phi)$ dependences at various values of ϵ was developed, based on the assumption that the confinement and attraction terms in the chemical potential μ_I of a polymer in an intrapore solution are independent of concentration. The concentration dependences $K(\phi)$ calculated by using the Flory or Huggins expressions for $\mu_I(\phi)$ are in good accord with the simulation results.

The detailed mapping of the concentration dependence of K in the vicinity of the critical energy ϵ_c shows that critical conditions for excluded volume chains may depend on concentration. The compensation point $K = 1$ was found at $\phi = 0.012$ irrespective of the pore width. The energy and entropy contributions to the free energy of confinement were calculated and the compensation of their values at critical condition was demonstrated. Further, partitioning within adsorptive pores was treated as a confined adsorption and the variations of the coefficient K were expressed as the adsorption isotherms. The concentration profiles $\phi_I(x)$ in the pore in equilibrium with the bulk solution were calculated for the adsorption and depletion regimes and their alteration with bulk concentration ϕ was elucidated.

Acknowledgment. The research was supported in part by the Grant Agency for Science (VEGA), Grants 2/7076/20 and 2/7056/20. Usage of the computational resources of the Computer Center of SAS is acknowledged.

References and Notes

- (1) Fleer, G. J.; Cohen Stuart, M. A.; Scheutjens, J. M. H. M.; Cosgrove, T.; Vincent, B. *Polymers at Interfaces*; Chapman & Hall: London, 1993.
- (2) Teraoka, I. *Prog. Polym. Sci.* **1996**, *21*, 89–149.
- (3) Casassa, E. F. *J. Polym. Sci., Polym. Lett. Ed.* **1967**, *5*, 773.

- (4) Davidson, M. G.; Suter, U. W.; Deen, W. M. *Macromolecules* **1987**, *20*, 1141–1146.
- (5) Cifra, P.; Bleha, T.; Romanov, A. *Polymer* **1988**, *29*, 1664–1668.
- (6) Bleha, T.; Cifra, P.; Karasz, F. E. *Polymer* **1990**, *31*, 1321–1327.
- (7) Wang, Y.; Teraoka, I. *Macromolecules* **1997**, *30*, 8473–8477.
- (8) Cifra, P.; Bleha, T.; Wang, Y.; Teraoka, I. *J. Chem. Phys.* **2000**, *113*, 8313–8318.
- (9) Cifra, P.; Bleha, T. *Polymer* **2000**, *41*, 1003–1009.
- (10) Cifra, P.; Bleha, T. *Macromolecules* **2001**, *34*, 605–613.
- (11) Chen, Z.; Escobedo, F. A. *Macromolecules* **2001**, *34*, 8802–8810.
- (12) de Gennes, P.-G. *Scaling Concepts in Polymer Physics*; Cornell University Press: Ithaca, NY, 1979.
- (13) Wang, Y.; Teraoka, I.; Cifra, P. *Macromolecules* **2001**, *34*, 127–133.
- (14) Cifra, P.; Wang, Y.; Teraoka, I. *Macromolecules* **2002**, *35*, 1446–1450.
- (15) Gorbunov, A. A.; Skvortsov, A. M. *Adv. Colloid Interface Sci.* **1995**, *62*, 31–108.
- (16) Skvortsov, A. M.; Gorbunov, A. A. *J. Chromatogr.* **1986**, *358*, 77–83.
- (17) Lin, N. P.; Deen, W. N. *Macromolecules* **1990**, *23*, 2947–2955.
- (18) Guttman, C. M.; DiMarzio, E. A.; Douglas, J. F. *Macromolecules* **1996**, *29*, 5723–5733.
- (19) Kosmas, M. K.; Bokaris, E. P.; Georgaka, E. G. *Polymer* **1998**, *39*, 4973–4976.
- (20) Berek, D. *Prog. Polym. Sci.* **2000**, *25*, 873–908.
- (21) Pasch, H.; Trathnigg, B. *HPLC of Polymers*; Springer-Verlag: Berlin, 1998.
- (22) Skvortsov, A. M.; Gorbunov, A. A.; Berek, D.; Trathnigg, B. *Polymer* **1998**, *39*, 423–429.
- (23) Lee, W.; Lee, H.; Lee, H. C.; Cho, D.; Chang, T.; Gorbunov, A. A.; Roovers, J. *Macromolecules* **2002**, *35*, 529–538.
- (24) Grull, H.; Shaulitch, R.; Yerushalimi-Rozen, R. *Macromolecules* **2001**, *34*, 8315–8320.
- (25) Snyder, L. R. In *High-Performance Liquid Chromatography*, 3rd ed.; Horvath, C., Ed.; Academic Press: New York, 1983; p 157.
- (26) de Joannis, J.; Park, C.-W.; Thomatos, J.; Bitsanis I. A. *Langmuir* **2001**, *17*, 69–77.
- (27) Thompson, A. P.; Glandt, E. D. *Macromolecules* **1996**, *29*, 4314–4323.
- (28) Satterfield, C. N.; Colton, C. K.; Turckheim, B. D.; Copeland, T. M. *AIChE J.* **1975**, *24*, 937.
- (29) Brannon, J. H.; Anderson, J. L. *J. Polym. Sci., Polym. Phys. Ed.* **1982**, *20*, 857.
- (30) Teraoka, I. *Macromolecules* **1996**, *29*, 2430.
- (31) Bleha, T.; Sychaj, T.; Vondra, R.; Berek, D. *J. Polym. Sci., Polym. Phys. Ed.* **1983**, *21*, 1903.
- (32) Post, A. J.; Glandt, E. D. *J. Colloid Interface Sci.* **1985**, *108*, 31–45.
- (33) Flory, P. J. *J. Chem. Phys.* **1942**, *10*, 51.
- (34) Huggins, M. L. *Ann. N.Y. Acad. Sci.* **1942**, *43*, 1.
- (35) Dickman, R. *J. Chem. Phys.* **1992**, *96*, 1516–1522.
- (36) Nies, E.; Cifra, P. *Macromolecules* **1994**, *27*, 6033–6039.
- (37) Gong, Y.; Wang, Y. *Macromolecules* **2002**, *35*, 7492–7498.
- (38) Pandey, R. B.; Michev, A.; Binder, K. *Macromolecules* **1997**, *30*, 1194–1204.

MA020808Z